Interface recombination velocity measurement in SiO_2/Si

© S. Ilahi, N. Yacoubi

Unité de Recherche de caractérisation photo-thermique
IPEIN. Universite de Carthage, La Tunisie.

(Получена 18 марта 2013 г. Принята к печати 13 июня 2013 г.)

The photothermal technique has been used in its orthogonal configuration in order to determine the interface recombination velocity between SiO_2 ultra-thin film and Si substrate. This investigation has been performed by studying the variation of the photothermal signal according to the square root modulation frequency of the pump light beam. A general one-dimensional theoretical model taking into consideration the nonradiative recombination process has been developed. The interface recombination velocity has been evaluated by fitting the experimental curves of the phase and normalized amplitude of the photo-thermal signal with the corresponding theoretical ones.
Key words: non-radiative lifetime, photo-thermal deflection, electronic parameters.

1. Introduction

As well known, SiO_2/Si covers wide range of application including metal−oxide semiconductor (MOS) and thin films Transistor (TFT) and solar cells. However, the interface recombination is a fascinating subject from both technological and fundamental aspects. Indeed, the interface recombination affects the efficiency of this kind of material. The growth conditions and the lattice mismatch between the SiO_2 layer and Si substrate are the main cause for dangling bands, impurities and defects which act as a nonradiative recombination centers for the photogenerated carrier in SiO_2/Si interface. Consequently, a tremendous effort [1–6] has been dedicated to study the interface states in SiO_2/Si and to evaluate the interface recombination velocity (IRV) that becomes an important electronic parameters. Then, several techniques have been used to measure the transport parameters by means of an adapted and accurate technique such as the photoluminescence [7], photoacoustic [8–10], photoreflectance [11] and photothermal radiometry [12–13]. Particularly the photothermal deflection technique (PTD) has proven a great versatility as a noncontactless, nondestructive and noninvasive method for evaluation of thermal and optical properties of materials [14–22]. It is worth to notice that PTD technique has been used to investigate the transport properties in silicon by D. Fournier et al [22] and more recently by Antia R. Warrier [23,24]. Recently, we have reported on a more general theoretical model taking into account of both thermal and electronic contribution in the PTD signal [25]. Furthermore, for the first time, the interface recombination velocity in SiO_2/Si has been evaluated, by means of PTD technique through fitting the experimental curves of amplitude and phase of the PTD signal to the corresponding theoretical ones versus square root modulation frequency.

2. Theory

The principle of PTD technique is shown in Fig. 1 where the sample is heated by a modulated light beam. The absorbed light generates electron-hole pairs that diffuse and recombine nonradiatively providing a heat through three fundamental process; namely intraband thermalization, bulk recombination and surface recombination. The thermal wave propagates into the sample and in the surrounding media inducing a refractive index gradient in the fluid that causes the deflection of a probe laser beam skimming the sample surface. As the incident light is assumed to be uniform and only the sample absorbs the light with an absorption coefficient α, so, a one dimensional treatment of the thermal wave is sufficient. Our theoretical model is based on the one-dimensional model proposed by D. Fournier et al. [22], except that in their model the probe beam crosses inside the sample while in our case the probe beam passes through the fluid in contact with the heated sample surface. In addition, they don't take into account of both fluid and backing in contact with the sample in the temperature expression. However, Anita R. Warrier et al [23,24] have taken into consideration the fluid and backing in the temperature expression, but they make several assumptions in their model linked to the sample properties. First, the sample is assumed thermally and optically thin (i. e. thermal and optical diffusion lengths exceed the layer thickness). The second assumption is applied to the minority carrier diffusion equation in which the material is in steady state. Furthermore, the first assumption prevents them to determine the electronic diffusion coefficient and it's valid for the case of bulk semiconductors. In the

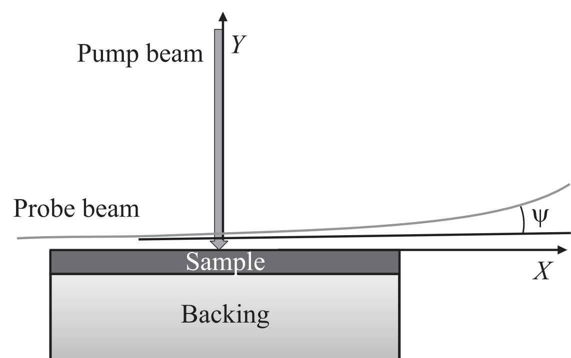

Figure 1. Schematic representative of Principle of PTD technique.

Meanwhile, in our work, we have taken into account the fluid and backing in the temperature expression and we have resolved the equation of minority carrier without doing any assumptions which make our model more general and adapted for one layer semiconductor (bulk or thin films) in contact with fluid and backing [25]. The theory is based on the resolution of minority carrier diffusion and heat equations.

2.1. Minority carrier diffusion equation

The carrier diffusion equation in the x direction in the general case may be written as:

$$\frac{\partial N(x,t)}{\partial t} = D\frac{\partial^2 N(x,t)}{\partial x^2} - \frac{N(x,t)}{\tau} + G, \quad (1)$$

where is $N(x,t)$ the photo-generated carriers density, D the electronic diffusion coefficient and (τ_{nr}) is the nonradiative lifetime of minority carriers and $G = \frac{\alpha I_0(1-R)}{2E}\exp(\alpha x)$ is the carriers generation rate. I_0 is the intensity of pump beam, α is the optical absorption coefficient, R is the reflectivity coefficient and E is the incident beam energy.

The general solution of equation (1) is:

$$N(x) = c\exp(ax) + d\exp(-ax) + \lambda\exp(\alpha x), \quad (2)$$

with

$$\omega = 2\pi F; \quad \lambda = \frac{b}{(\alpha^2 - a^2)}, \quad b = \frac{-\alpha I_0(1-R)}{2ED}$$

and

$$l_{\text{diff}} = \frac{1}{a} = \left(\frac{i\omega + \frac{1}{\tau}}{D}\right)^{-1/2}$$

is the electronic diffusion length; c and d are constants that can be determined by applying the boundaries conditions:

$$D\frac{\partial N}{\partial x}(x=0) = SN(x=0), \quad (3)$$

$$N(x \prec -l) = 0, \quad (4)$$

S is the surface recombination velocity.

Then, we obtain:

$$d = -\lambda\exp\big(-l(a+\alpha)\big), \quad (5)$$

$$c = \frac{-\lambda\exp\big(-l(a+\alpha)\big)(S+aD)}{aD-S} + \frac{\lambda(S-\alpha D)}{aD-S}. \quad (6)$$

2.2. Heat diffusion equation

The equations of heat diffusion in different media are:

$$\frac{\partial^2 T_f}{\partial x^2} - \sigma_f^2 T_f = 0, \quad \text{if} \quad 0 \le x \le l_f, \quad (7)$$

$$\frac{\partial^2 T_s}{\partial x^2} - \sigma_s^2 T_s = Q(x,t), \quad \text{if} \quad -l \le x \le 0, \quad (8)$$

$$\frac{\partial^2 T_b}{\partial x^2} - \sigma_b^2 T_b = 0, \quad \text{if} \quad -l_b - l \le x \le l. \quad (9)$$

Where $\sigma_i = \frac{(1+i)}{\mu_i}$ and $\mu_i = \left(\frac{D_i}{\pi F}\right)^{1/2}$ is the thermal diffusion length of the i medium ($i = f, s, b$ respectively the fluid f, the sample s and the backing b), and F is the modulation frequency of the pump beam. In fact $Q_{(x,t)}$ represents the heat source term which is the sum of three fundamental heats sources given as follow. The first source $Q_{\text{th}(x,t)} = \alpha I_0(1-R)\left(\frac{\Delta E}{E}\right)\exp(\alpha x)$ is due to the thermalization of the carriers where the excess energy $\Delta E = E - E_g$ is given in the crystal lattice by interaction with phonons. The second source $Q_{\text{bulk}(x,t)} = \frac{E_g}{\tau K_s} N_{(x,t)}$ is due to the bulk recombination of photogenerated carriers, after diffusion. Finally, the third source $Q_{\text{Sur}(x,t)} = SE_g N_{(x,t)}$ is caused by the recombination at the sample surface where recombination is particularly high due to defects and dangling bonds.

The periodic solutions in the different media are given as follow:

— In the fluid $\quad T_f = T_0\exp(-\sigma_f x), \quad (10)$

— In the sample $\quad T_s = u\exp(\sigma_s x) + v\exp(-\sigma_s x) + m\exp(ax) + n\exp(-ax) + (q+A)\exp(\alpha x), \quad (11)$

— In the backing $\quad T_b = B\exp\big(\sigma_b(l+x)\big), \quad (12)$

where T_0, u, v, m, n, q, A and B are complex constant which are determined using the continuity of temperature and heat flow at the different interfaces:

$$T_f(0) = T_s(0), \quad (13)$$

$$-K_f\frac{\partial T_f}{\partial x}(0) = -K_s\frac{\partial T_s}{\partial x}(0) + SE_g N(0), \quad (14)$$

$$T_s(-l) = T_b(-l), \quad (15)$$

$$-K_s\frac{\partial T_s}{\partial x}(-l) = -K_b\frac{\partial T_b}{\partial x}(-l). \quad (16)$$

By solving theses equations one can obtain the expression (17) of the periodic temperature rise T_0 at the sample surface:

$$T_0 = \frac{\left\{\begin{array}{l} (1-f)\exp(-\sigma_s x)\Big[m(1+a_s) + n(1-a_s) + (r+1)(q+A) \\ -\frac{SE_g}{K_s\sigma_s}N(0)\Big] - (1+f)\exp(\sigma_s x)\Big[m(1-a_s) + n(1+a_s) \\ +(1-r)(q+A) - \frac{SE_g}{K_s\sigma_s}N(0)\Big] + 2m(f-a_s)\exp(-al) \\ +2n(f+a_s)\exp(+al) + 2(1+A)(f-r)\exp(-\alpha l) \end{array}\right\}}{[(1-f)(1-g)\exp(-\sigma_s l) - (1+f)(1+g)\exp(\sigma_s l)]}, \quad (17)$$

$$a_s = \frac{a}{\sigma_s}, \quad e = \frac{E_g}{\tau K_s}, \quad n = \frac{ed}{a^2 - \sigma_s^2},$$

$$r = \frac{\alpha}{\sigma_s}, \quad m = \frac{ec}{a^2 - \sigma_s^2}, \quad f = \frac{K_f\sigma_f}{K_s\sigma_s},$$

$$g = \frac{K_s\sigma_s}{K_b\sigma_b}, \quad q = \frac{e\lambda}{\alpha^2 - \sigma_s^2} \quad \text{and} \quad A = \frac{\alpha I_0(1-R)(E-E_g)}{2EK_s(\alpha^2 - \sigma_s^2)}.$$

The expression of probe beam deflexion is given by J.C. Murphy et al. [26]:

$$\psi = \frac{L}{n}\frac{dn}{dT}\sigma_f T_0 \exp(-\sigma_f x_0), \tag{18}$$

n is the refractive index, L is the sample length, ψ is complex number written as $\psi = |\psi| \exp(\phi)$ where $|\psi|$ is the amplitude and ϕ the phase; x_0 is the distance between the probe beam axis and the sample surface ($x_0 \approx 60\,\mu$m).

3. Experimental details

The experimental set-up is described elsewhere [25] where the sample (Fig. 2) is heated by mechanically chopped light produced by a halogen lamp. He−Ne-laser probe beam of $100\,\mu$m diameter skimming the sample surface at x_0 distance is deflected. The deflection is detected by a position photodetector linked to a lock in amplifier. The obtained photothermal signal has two compounds: amplitude and phase. A computer reads the values of amplitude and phase and draws their variation versus square root frequency. Thus, the samples under study were grown on p-type silicon at temperatures around of 1000°C presenting respectively a resistivity and thickness of $0.2\,\Omega$cm and $400\,\mu$m. A 5 nm of ultrathin SiO_2 layer is deposed in Si substrate by thermal oxidation at 1100°C.

It is worth to indicate that the expression (18) allows to evaluate the IRV (S_i) in SiO_2/Si assuming that the light cannot be absorbed in SiO_2 film layer. The Fig. 3 shows the amplitude (Fig. 3, a) and phase (Fig. 3, b) of the PTD signal for different values of IRV in order to show the great sensitivity of the PTD signal on the IRV. In other hand, the dependence of the amplitude and phase on the frequency is described in detail in the one layer model proposed elsewhere [22,23]. Moreover, two regimes are identified: the first is purely thermal behavior that occurs at low frequency regime < 100 Hz inducing a rapid decrease in the amplitude of the PTD signal. This behavior is explained by the carrier thermalization. The second is an electronic

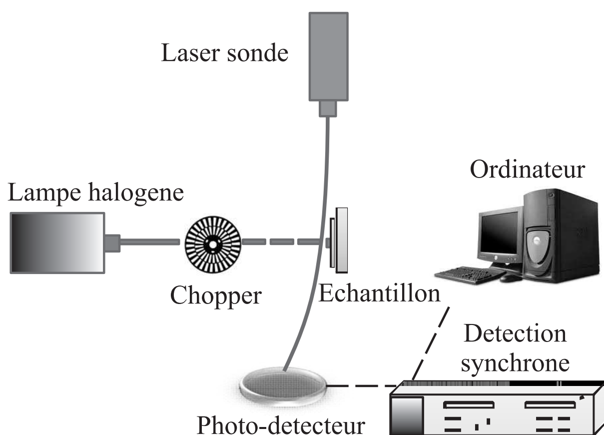

Figure 2. Schematic experimental setup of the PTD technique.

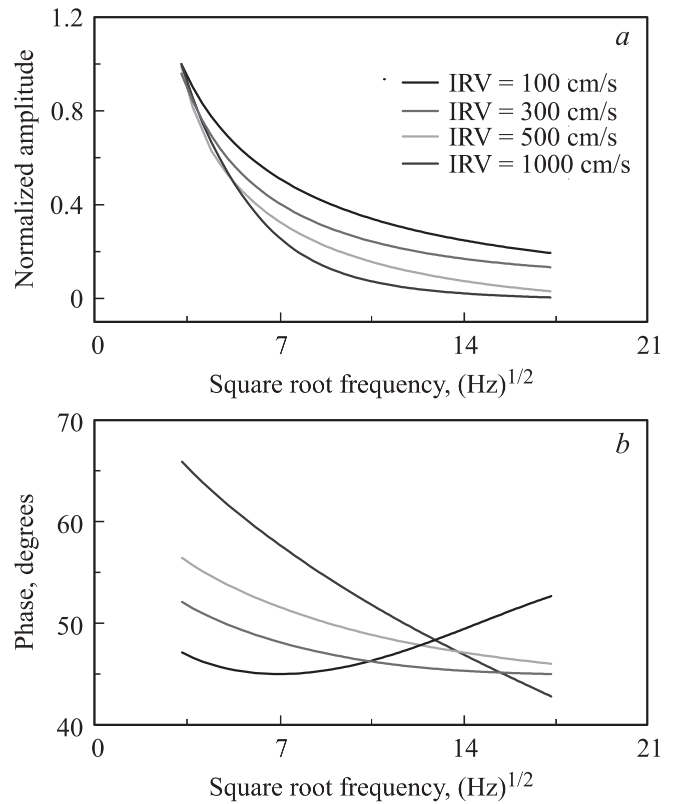

Figure 3. Normalized amplitude (a) and phase (b) of theoretical PTD signal versus square root modulation frequency for different values of IRV.

behavior that occurs in the high frequency > 100 Hz and described by a slow decrease in the amplitude. Furthermore, we have fitted simultaneously the amplitude and phase of PTD signal in order to ensure the uniqueness of the extracted value. The other parameters used in the fitting procedure are reported elsewhere [22]. The Fig. 4 shows the experimental amplitude (Fig. 4, a) and phase (Fig. 4, b) of the photothermal signal and the corresponding theoretical ones. Thus, the best fit is realized between experimental and theoretical phase and amplitude curves according to the modulation frequency given a moderate value of 1240 ± 10 for S_i. For cons, the value presented by T. Ikari et al. [28] using reflection microscopy photo-thermal is a little high in the vicinity of 2500 cm/s. Then, we can deduce the rate of carrier recombination at the interface varies greatly depending on defect density. The growth conditions and the lattice mismatch between the SiO_2 layer and the silicon substrate is the mainly cause for the defects at the interface. In addition, these results agree well with that reported in [29] which indicates that S_i varies from a few tens of cm/s to 104 m/s depending on the oxidation and annealing temperature and affected by the state of the oxide-silicon. As well know, the P_b centers designed as $^{\bullet}\mathrm{Si} \equiv \mathrm{Si}_3$, is the originate of the defects in the SiO_2/Si interface [30–32]. Then, IRV is related to defect density through SRH model $d/S_i = 1/\sigma_e v_{\mathrm{th}} N_d$, σ_e is the electron capture cross section

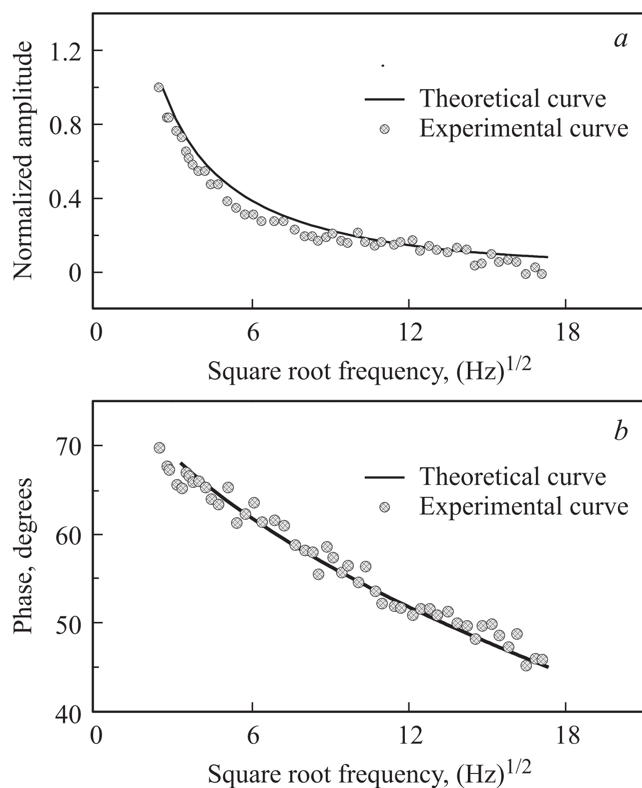

Figure 4. Experimental (dots) and theoretical (line) amplitude and phase of the PTD signal according to square root modulation frequency for SiO_2/Si.

estimated $5 \cdot 10^{-16}\,\mathrm{cm}^2$ [33], v_{th} is the carrier thermal velocity 10^7 cm/s [34] and d is the substrate thicknesses. In fact, we have found that the defect density have almost equal to $62 \cdot 10^{15}\,\mathrm{cm}^{-3}$.

In summary, a one layer theoretical model applied for photothermal deflection technique has been improved for interface recombination investigation. We have determined accurately the interface recombination velocity by fitting the experimental curves of the phase and normalized amplitude of the photothermal signal by the corresponding theoretical ones. The obtained values are a good agreement with that reported in literature which shown the sensitivity of the technique and the reliability of the model for applications in semiconducting structures.

References

[1] M.L. Reed, J.D. Plummer. J. Appl. Phys., **63** 5776 (1988).
[2] T.W. Hickmott. J. Appl. Phys., **48**, 723 (1977).
[3] Y. Nissan-Cohen. Appl. Surf. Sci., **39** 511 (1989).
[4] L. Polignano, G. Ferroni, A. Sabbadini, G. Valentini, G. Queirolo. J. Non-Cryst. Sol., **216**, 88 (1997).
[5] N. Stein, H. Röppischer. Phys. Status Solidi, **123** (1), 139 (1991).
[6] T. Ikari, A. Fukuyamaa, T. Murata, M. Suemitsu, N. Haddad, V. Reita, J.P. Roger c, D. Fournier. Mater. Sci. Engin. B, **124–125**, 345 (2005).
[7] D.H. Baek, S.B. Kim, D.K. Schroder. J. Appl. Phys., **104**, 054 503 (2008).
[8] M.D. Dramicanin, Z.D. Ristowski, P.M. Nikolic, D.G. Vasiljevic, D.M. Todorovic. Phys. Rev. B, **51** 20 (1995).
[9] I. Riech, M.L. Gomez-Herrera, P. Dıaz, J.G. Mendoza-Alvarez, J.L. Herrera-Perez, E. Marin. Appl. Phys. Lett., **79** (13), 7 (2001).
[10] I. Reich, P. Dıaz, T. Prutskij, J. Mendoza, H. Vargas, E. Marin. J. Appl. Phys., **86** (11), 1 (1999).
[11] B.C. Forget, D. Fournier, V.E. Gusev. Appl. Surf. Sci., **63** (255–159) (1993).
[12] A. Mandelis, A. Othonos, C. Christofides, J. Boussey-Said. J. Appl. Phys., **80** (9), 1 (1996).
[13] M. Nestoros, Y. Karmiotis, C. Christofides. J. Appl. Phys., **82** (12), 15 (1997).
[14] W.B. Jackson, N.M. Amer, A.C. Boccara, D. Fournier. (1981-04-15). Appl. Optics, **20** (8), 1333 ().
[15] S. Ilahi, F. Saidi, R. Hamila, N. Yacoubi, L. Auvray, H. Maaref. Current Appl. Phys., **13** 610 (2013).
[16] A.C. Boccara, D. Fournier, Badoz. Appl. Phys. Lett., **36**, 130 (1979).
[17] J.C. Murphy, L.C. Aamodt. J. Appl. Phys., **51**, 4580 (1980).
[18] L.C. Aamodt, J.C. Murphy. J. Appl. Phys., **49**, 3036 (1978).
[19] A. Mandelis. J. Appl. Phys., **54**, (6), 3404 (1983).
[20] R.E. Wagner, A. Mandelis. Phys. Rev. B, **38**, 9920 (1988).
[21] *Photoacoustic and Thermal Wave Phenomena in Semiconductors*, ed. by A. A. Mandelis (Elsevier, N. Y., 1987).
[22] D. Fournier, C. Boccara, A. Skumanich, M. Nabil, Am. J. Appl. Phys., **59**, 3 (1986).
[23] Anita R. Warrier, Tina Sebastian, C. Sudha Kartha, K.P. Vijayakumar. J. Appl. Phys., **107**, 073 701 (2010).
[24] Anita R. Warrier, K.G. Deepa, Tina Sebastian, C. Sudha Kartha, K.P. Vijayakumar. Thin Sol. Films, **518**, 1767. (2010).
[25] S. Ilahi, F. Saadalah, N. Yacoubi. Appl. Phys. A DOI 10.1007/s00339-012-7242-6.
[26] L.C.M. Miranda. Appl. Optics, **21**, 2923 (1982).
[27] J.C. Murphy, L.D. Aamodt. J. Appl. Phys., **9**, 51 (1980).
[28] T. Ikari, A. Fukuyama, T. Murata, M. Suemitsu, N. Haddad, V. Reita, J.P. Roger, D. Fournier. Mater. Sci. Engin. B, **124–125** 345 (2005).
[29] Polignano, G. Ferroni, A. Sabbadini, G. Valentini, G. Queirolo. J. Non-Cryst. Sol., **216**, 88 (1997).
[30] E.H. Poindexter, P.H. Caplan, B.E. Deal, G.J. Gerardy. *The physics and chemistry of* SiO_2 *and* Si–SiO_2 *interfaces* (N. Y., Plenum, 1988) p. 299.
[31] J. Rpbertson, Adv. Phys., **32**, 361 (1983).
[32] T. Ando, A.B. Fowler, F. Stern. Rev. Mod. Phys., **54**, 437 (1982).
[33] S. Altındal, H. Kanbur, I. Yucedag, A. Tataroglu. Microelectron. Engin., **85**, 1495 (2008).
[34] E. Simoen, C. Clarys, R. Falster, C. Masure, P. Stallhorfer. Hight purty silicon. ECS Transaction, p. 148.

Редактор Т.А. Полянская